Supplementary file

La/Fe bimetallic MOFs derived p-$LaFeO_3$/n-CdS heterojunction: An efficient photocatalytic degradation of organic contaminants and adsorption isotherms

Mohammad Saud Athar, Azam Khan, Iftekhar Ahmad, and Mohammad Muneer

Department of Chemistry; Aligarh Muslim University; Aligarh 202002, India.
Email: m.muneer.ch@amu.ac.in, readermuneer@gmail.com
Tel. +919897279787, +91-571-2700920

2.5 Materials characterization

The synthesized samples underwent comprehensive characterization using a range of standard analytical techniques. X-ray diffraction (XRD) was employed to analyze the crystal structure and phase of the samples. UV-Vis diffuse reflectance spectroscopy (DRS) was utilized to investigate their optical properties. Fourier transform infrared spectroscopy (FTIR) was performed to study the molecular vibrations and functional groups present in the materials. Scanning electron microscopy (SEM) coupled with energy dispersive spectroscopy (EDS) provided information on the morphology and elemental composition of the samples. Transmission electron microscopy (TEM) was employed to obtain the internal morphology of the as-synthesized catalyst. X-ray photoelectron spectroscopy (XPS) was used to determine the elemental analysis and chemical states of the synthesized materials. Brunauer Emmett Teller (BET) analysis was used to determine the surface area, pore width and pore volume of the synthesized materials. For the XRD analysis, an X-ray beam diffractometer equipped with a graphite monochromatic copper radiation source was employed with an operating at a voltage of 30 kV and a current of 15 mA. The measurements were conducted between 5 and 80 ^{0}C with an output speed of 10^0 /min. UV-Vis diffuse reflectance spectroscopy was performed using a Perkin Elmer Lambda 35 spectrophotometer, which allows for the measurement of the optical properties of the synthesized material. To analyze the

photoluminescence spectra, a fluorescence spectrometer (Perkin Elmer LS 55) was employed. The Fourier transform infrared spectra were recorded using a Perkin Elmer Spectrum 2 spectrophotometer with KBr as a reference material. For elemental analysis and determination of chemical states, the XPS-AES Module with Ar ion and C60 sputter guns was utilized. This analysis was performed using the PHI 5000 Versa Probe II supplied by FEI Inc. To visualize the morphology and purity of the synthesized materials, SEM (JEOL JSM-6510LV) was employed and Transmission electron microscopy (TEM) images of the catalyst were obtained using a JEOL-JEM 2100 microscope operating at an accelerating voltage of 120 kV.

2.6 Measurement of photocatalytic activity

The potential applicability of the photocatalyst was examined by observing the degradation of dyes, rhodamine (RhB), congo red (CR) and antibiotics tetracycline (TC), oxytetracycline (OTC) in an immersion well photochemical reactor made of pyrex glass in aqueous suspension under visible light (using a 500 W halogen lamp with an average light intensity of 9500 lumens) irradiation with the continuous bubbling of air. The concentration of compounds for irradiation experiments was fixed as 10 ppm (dyes) and 20 ppm (ciprofloxacin drug). An aqueous solution of the compound (180 ml) was taken in the standard photochemical reactor and the synthesized catalyst (1g/L) was dispersed in the solution and sonicated for 10 min and stirred for 30 min in the dark to achieve the adsorption-desorption equilibration. The solution was then irradiated with visible light with proper cooling and stirring. The samples (5 mL) were collected at various time intervals and centrifuged at 6000 rpm to extract the catalyst from the sample mixture. The photodegradation was monitored by measuring absorption at their lambda max, i.e. RhB (553 nm), CR (496 nm) and TC (360 nm), OTC (380 nm) using a Perkin Elmer Lambda 35 UV-Vis spectrophotometer. Concentration was determined from the calibration curve using absorbance

values of UV-vis spectrophotometer. The catalyst's photodegradation efficiency was measured using the following equation (1):

$$\text{Degradation efficiency} = (C_0\text{-}C_t)/C_0 \times 100 \quad (1)$$

Where C_0 is the initial pollutant concentration at the adsorption-desorption equilibrium, and C_t is the final pollutant concentration at the time of irradiation.

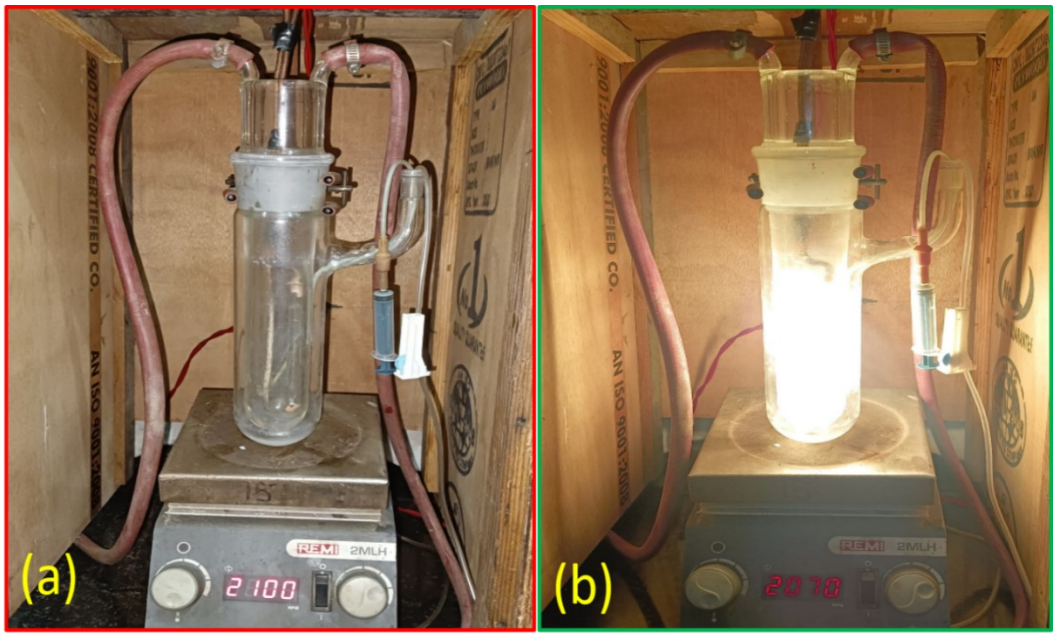

Fig S1 Photocatalytic reactor setup with inner and outer jacket for the degradation study **(a)** lamp off **(b)** lamp on with proper colling and stirring.

2.7 Trapping experiment

The main reactive species involved in the degradation of RhB over 15 LC heterojunction photocatalyst were recognized through trapping experiments. For this experiment, irradiations were carried out under similar conditions in the presence of various scavenger such ae (BQ), isopropyl alcohol (IPA), Na_2-EDTA to trap different species like, superoxide radical anion,

hydroxyl radical and hole. The reaction conditions were kept same as those in the photocatalytic activity experiments besides the scavengers were added before the addition of the catalyst. The concentration of scavengers was fixed as 2 mM, and the reaction was spectrophotometrically followed by monitoring the change in dye absorption as a function of irradiation time. Also, the hydroxyl radicals formed in the reaction medium were accessed via quantitative estimation using the terephthalic acid photoluminescence probe method. For this, the desired amount of 15LC heterojunction photocatalyst was properly suspended through sonication in an aqueous NaOH solution (2×10^{-3} M) and terephthalic acid (5×10^{-4} M). On excitation at 330 nm, the hydroxyl radicals generated combines with terephthalic acid to produce a fluorescent adduct (2-hydroxy terephthalic acid), which was monitored spectrofluorimetrically. It could be seen from the figure that the peak intensity is slightly increased with increasing illumination time, which confirms partial involvement of •OH radicals in the photocatalytic process.

2.8 Electrochemical analysis

The electrical measurements of different samples were performed using an LCR meter by making composite pellets with a thickness of 0.2 cm. For better electrical conductivity between the sample and electrodes, the pellets were coated with silver paste. AC impedance measurements were carried out using the pellet over a frequency range of 20 Hz -1 MHz at various temperatures under an air atmosphere.

3.6 BET analysis

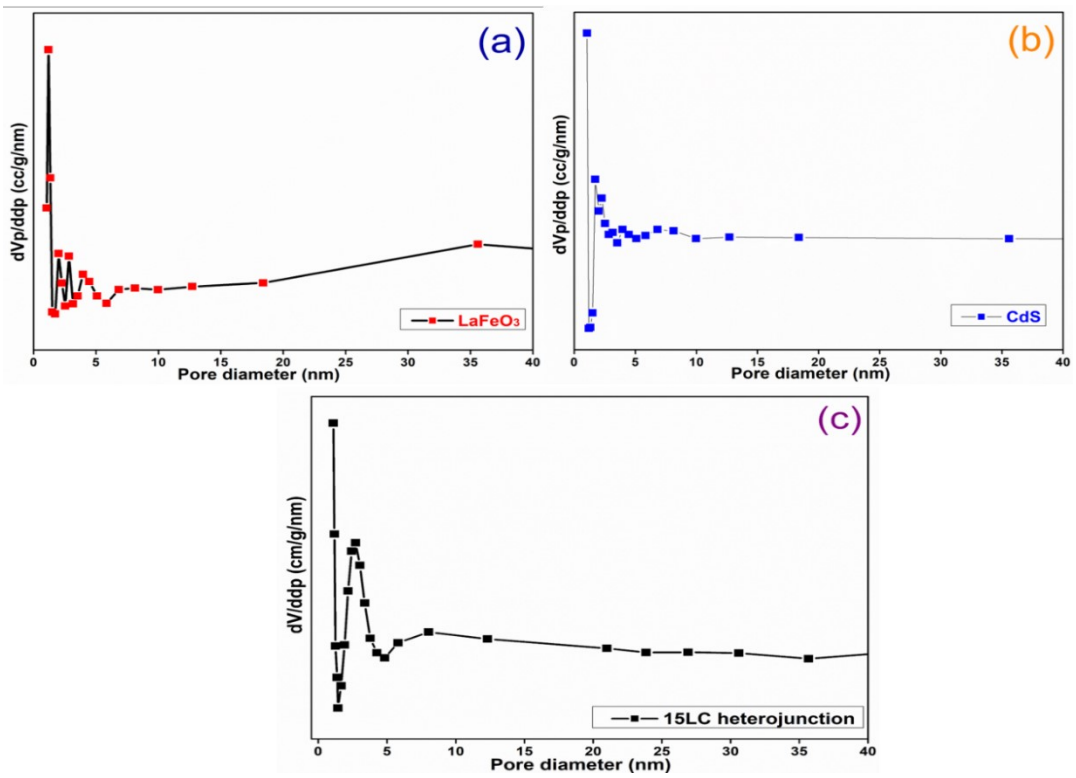

Fig S2 Pore size (diameter) distribution curve of pure **(a)** $LaFeO_3$, **(b)** CdS and **(c)** 15 LC heterojunction material.

3.8 TEM analysis

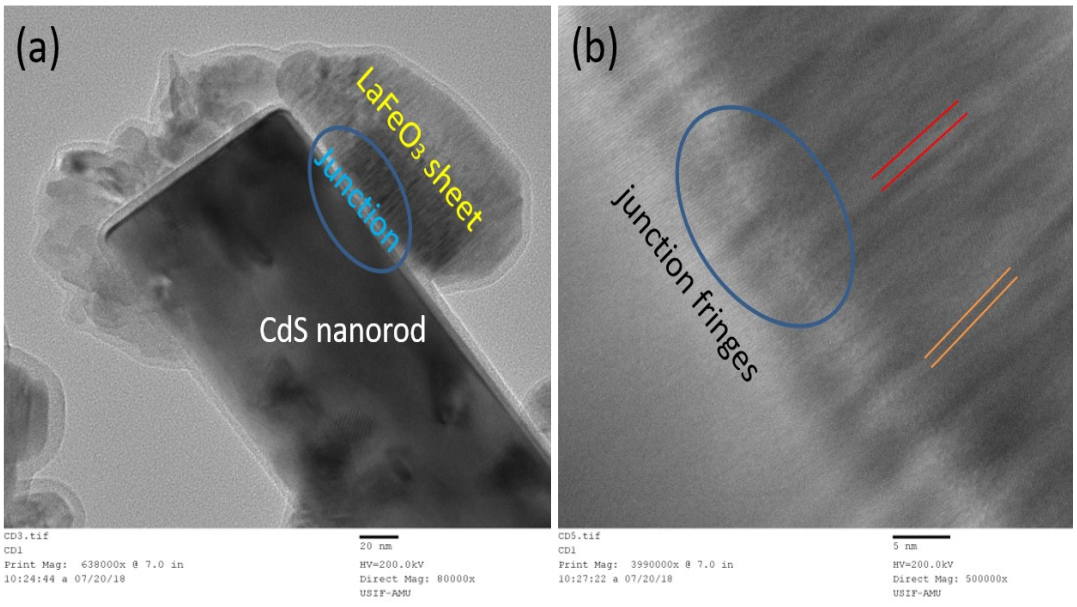

Fig S3 TEM images of 15LC heterojunction, at low **(a)** and high magnification **(b)**.

3.9 TGA analysis

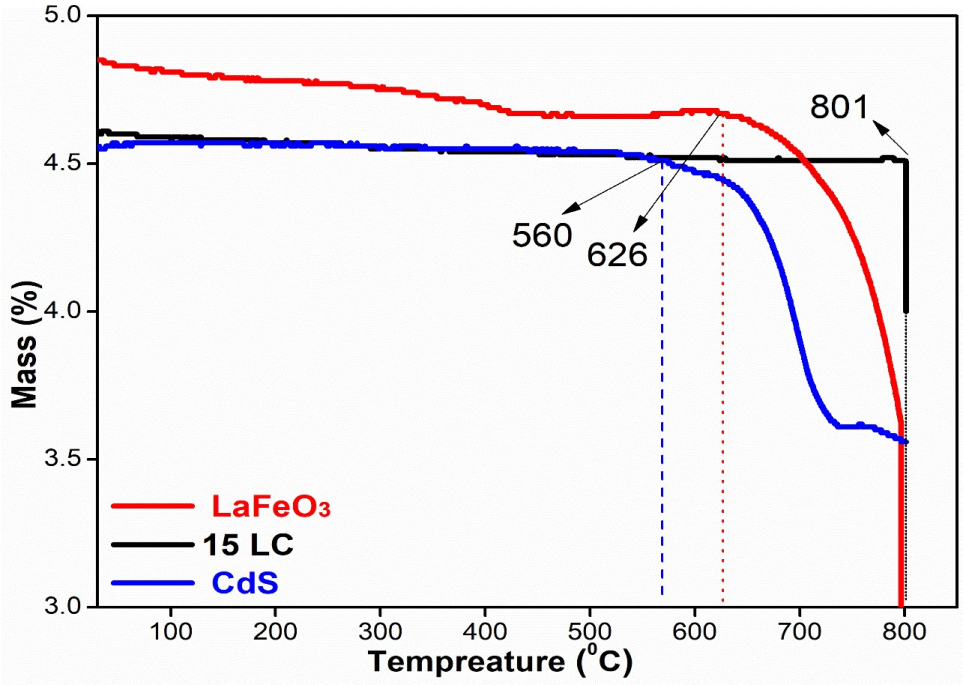

Fig S4 TGA spectra of as-prepared pure CdS, $LaFeO_3$ and 15 LC heterojunction material.

4.0 Photocatalytic degradation

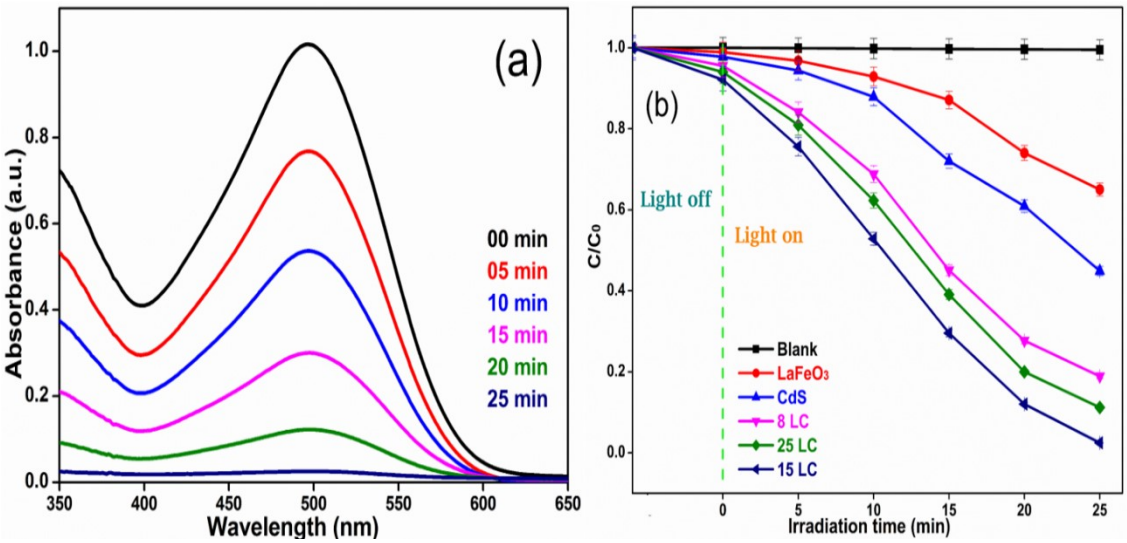

Fig S5 (a) Absorbance change of CR dye over 15 LC heterojunction (catalyst dosage = 1 g/L) and **(b)** change in concentration of CR (10 ppm, 180 mL) with time in the absence and presence of catalysts under visible light irradiation.

Table S1. Comparative study of the degradation of organic pollutants using 15 LC composite materials with earlier reported resuts.

Type of pollutants	Initial concentration of pollutants (mg/L)	Photocatalyst	Photocatalyst concentration (g/L)	Experimental condition	Time (min)	Degradation (%)	References
RhB	10	$LaFeO_3$/CdS	1	500W halogen lamp	30	98	Current Study
CR	10	$LaFeO_3$/CdS	1	”	25	99	’’
CF	30	$LaFeO_3$/CdS	1	”	100	96	’’
RhB	10	$LaFeO_3$/g-C_3N_4/$BiFeO_3$	1	Xenon lamp	~	97	[6]
CR	10	$LaFeO_3$/g-C_3N_4	1.5	300W xenon lamp	180	85	[41]
MB	10	WO_3/$AgInS_2$	1	Visible light source	180	90	[53]
2,4-Dichloro Phenol	10	ZnO/Bi-$LaFeO_3$	2.5	Xenon lamp 150 W	120	77	[38]
Phenol	~	p-$LaFeO_3$/n-ZnO	1.5	Visible light source	180	95	[5]

4.2 Adsorption isotherms

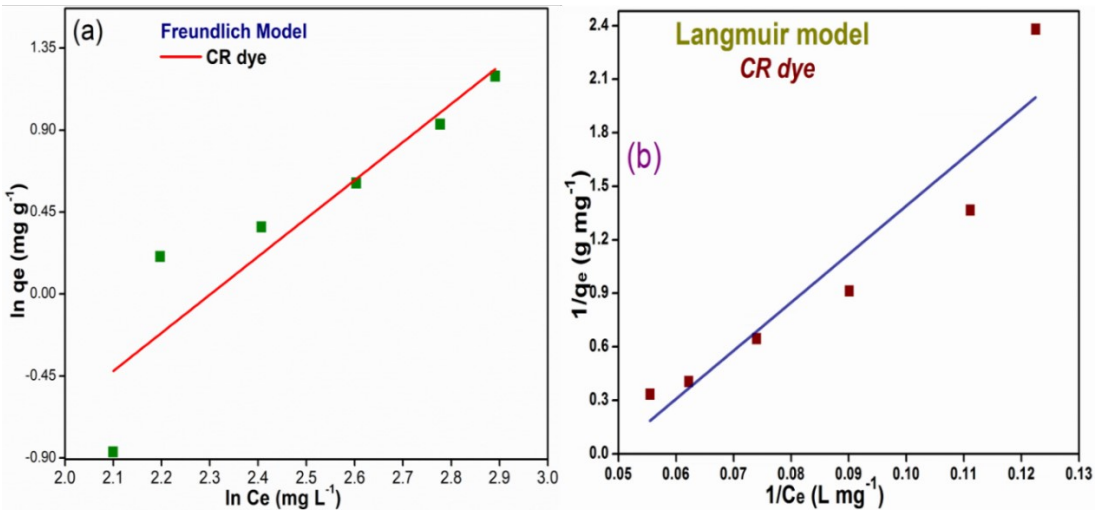

Fig S6 Adsorption isotherm for removing CR dye over 15 LC heterojunction **(a)** Freundlich and **(b)** Langmuir.

4.3 Photocatalysis of 4-nitrophenol over synthesized catalyst [15 $LaFeO_3$-CdS (15LC)]

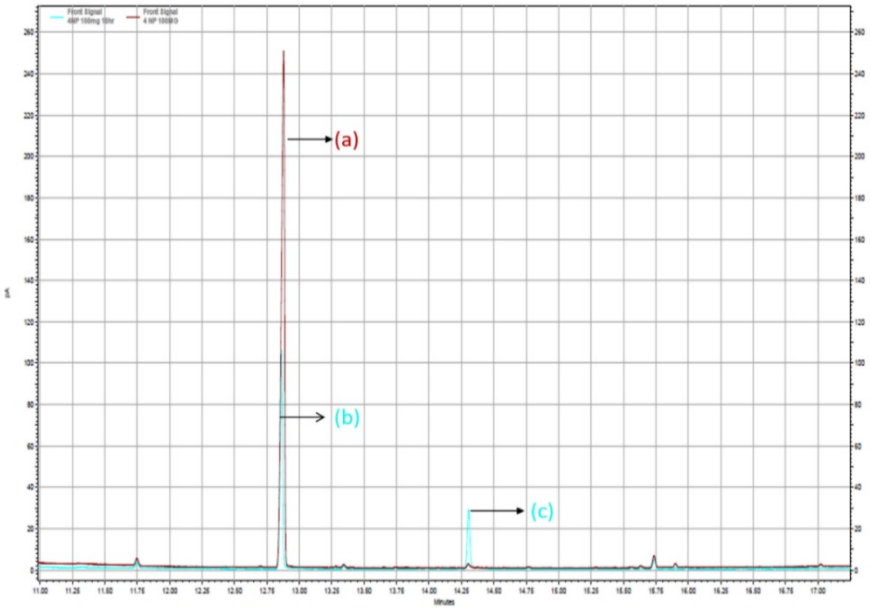

Fig S7 GC analysis of 4-Nitrophenol after 10 h irradiation using 15 LC photocatalyst in methanolic solution under N_2 environment.

4.4 TOC & HPLC

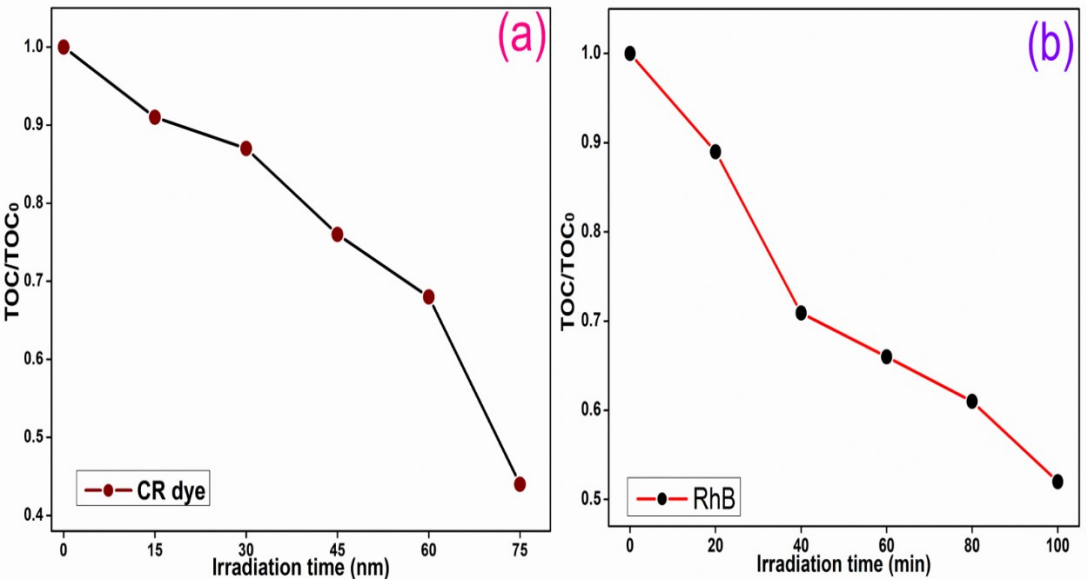

Fig S8 TOC/TOC_0 vs irradiation time of **(a)** CR and **(b)** RhB in the presence of 15 LC heterojunction photocatalyst (1 g/L) with 50 ppm concentration, in 180 ml photoreactor.

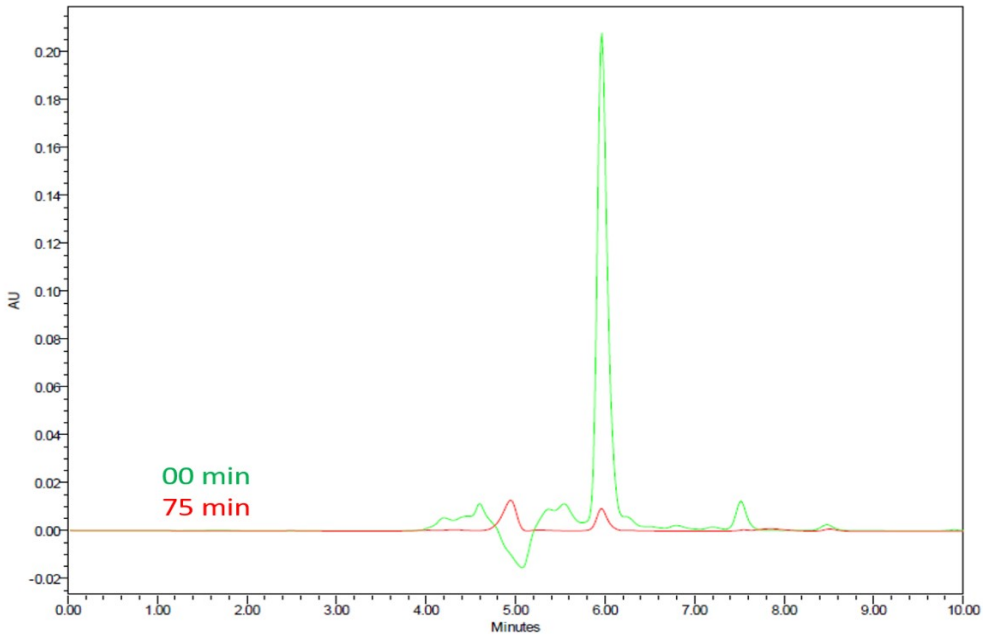

Fig S9 HPLC chromatogram of paracetamol (30 ppm) over 15 LC heterojunction under visible light irradiation in an aqueous suspension.

4.5 EIS & CV analysis

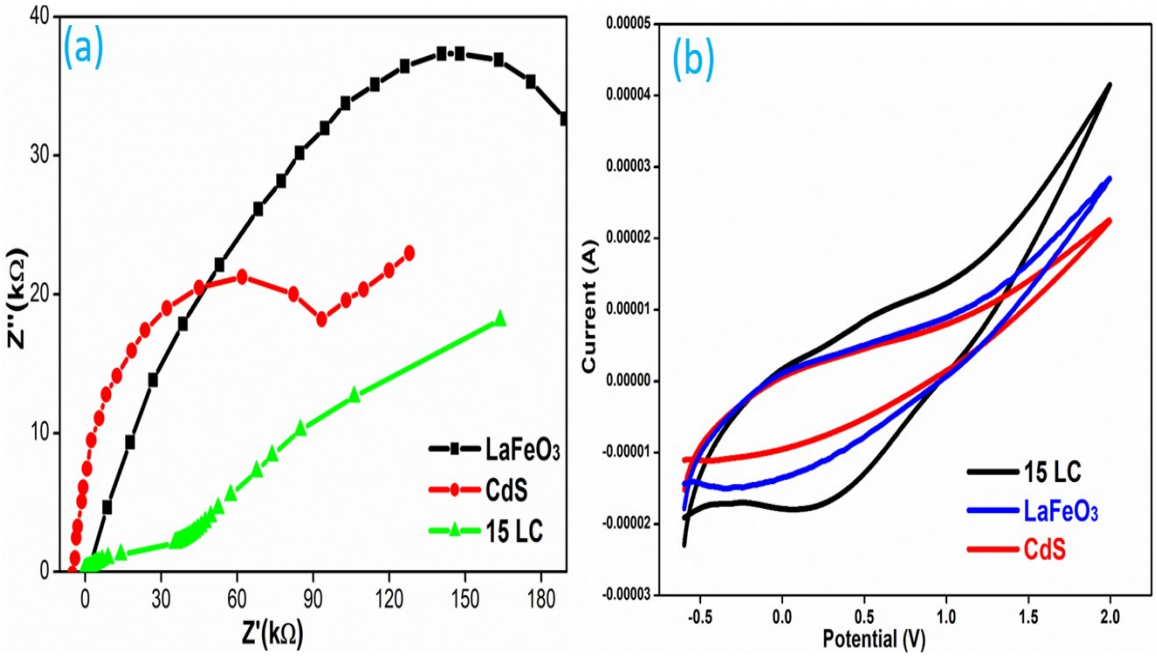

Fig S10 (a) Electrochemical impedance spectra (Nyquist plots) of the as-synthesized pure $LaFeO_3$, CdS and 15 LC heterojunction and **(b)** CV results of CdS, $LaFeO_3$ and 15LC photocatalyst in a solution of 5 mM $[Fe(CN)_6]^{3-/4-}$ containing 0.1 M KCl.

4.6 Effect of different pH on photocatalytic degradation

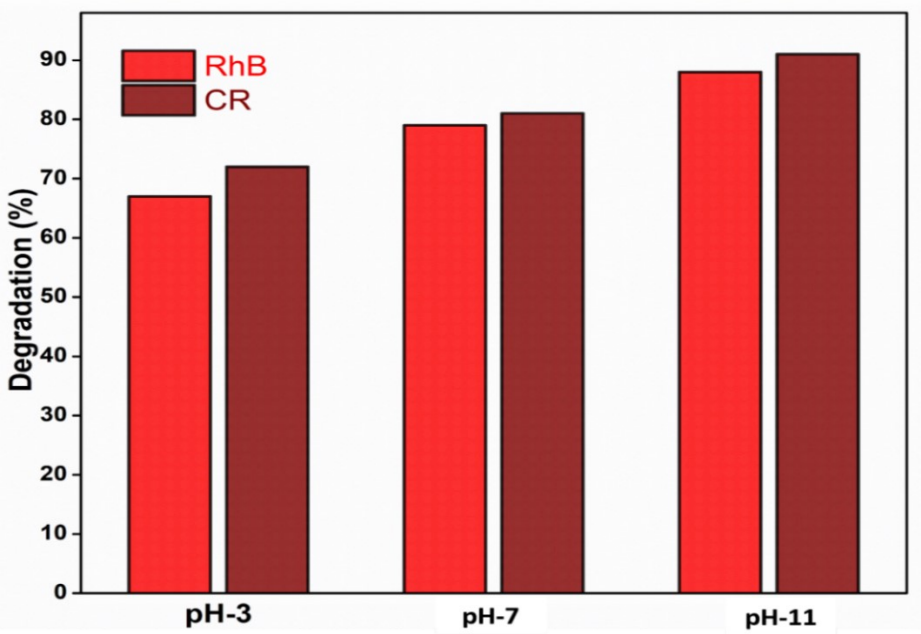

Fig S11 Degradation percentage response of RhB and CR dye at different pH (3, 7 and 11).

4.7 Stability of catalyst

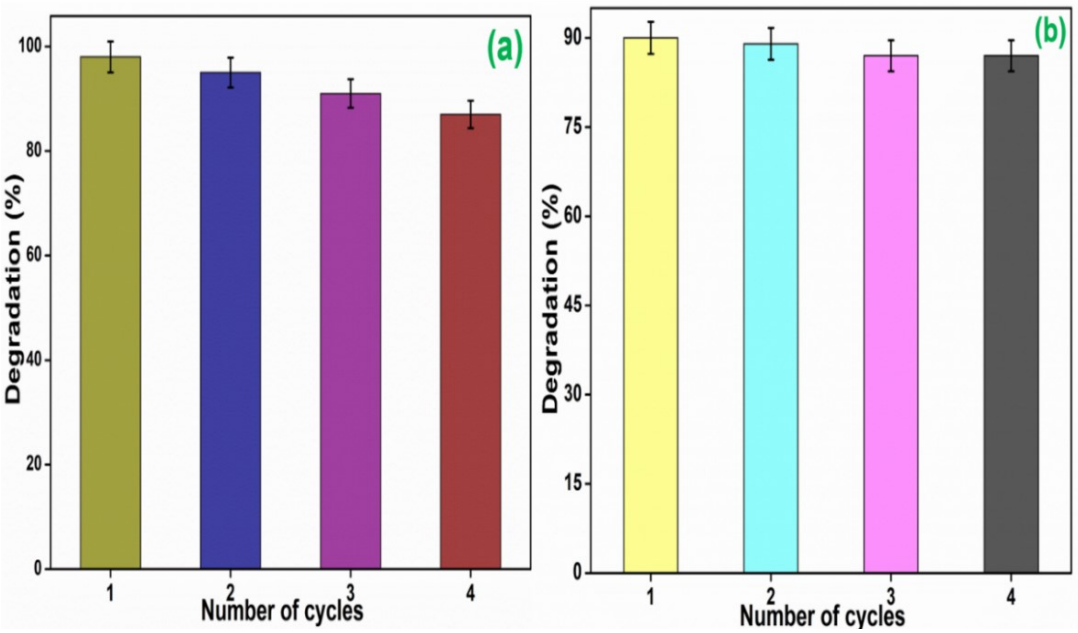

Fig S12 (a) Recyclability of 15 LC heterojunction photocatalyst towards photocatalytic degradation of CR dye **(b)** CF drug for four successive runs in aqueous suspension.

5.0 Quenching & ROS estimation

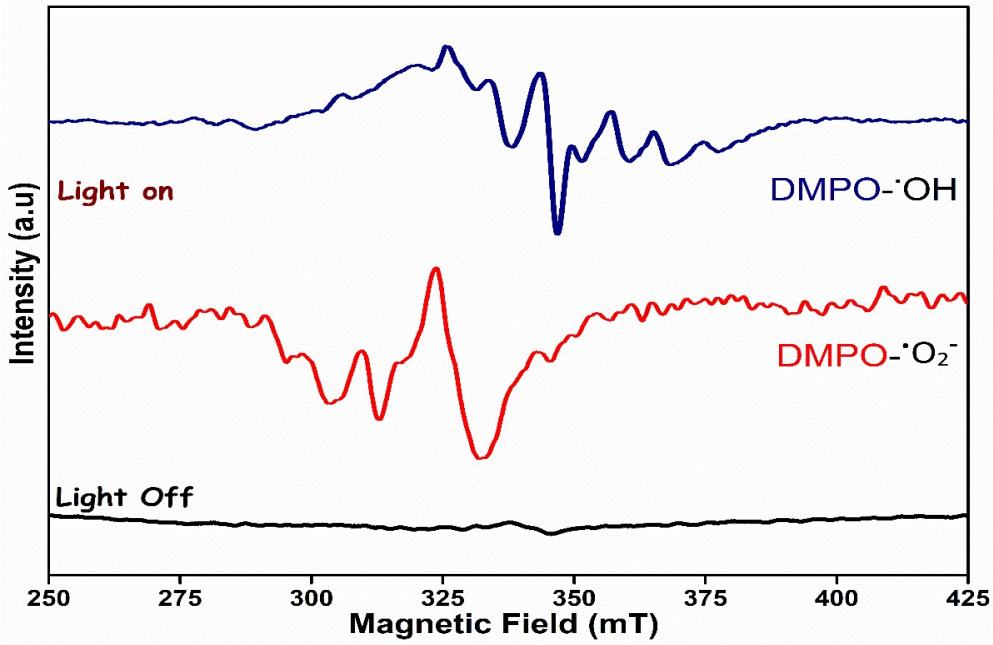

Fig S13 Spin trapping ESR spectra of 15 LC heterojunction using DMPO, in methanol for DMPO-$O_2^{\bullet-}$and in H_2O for DMPO-$^{\bullet}OH$.

6.0 Photocatalytic degradation mechanism (Mott-Schottky plot)

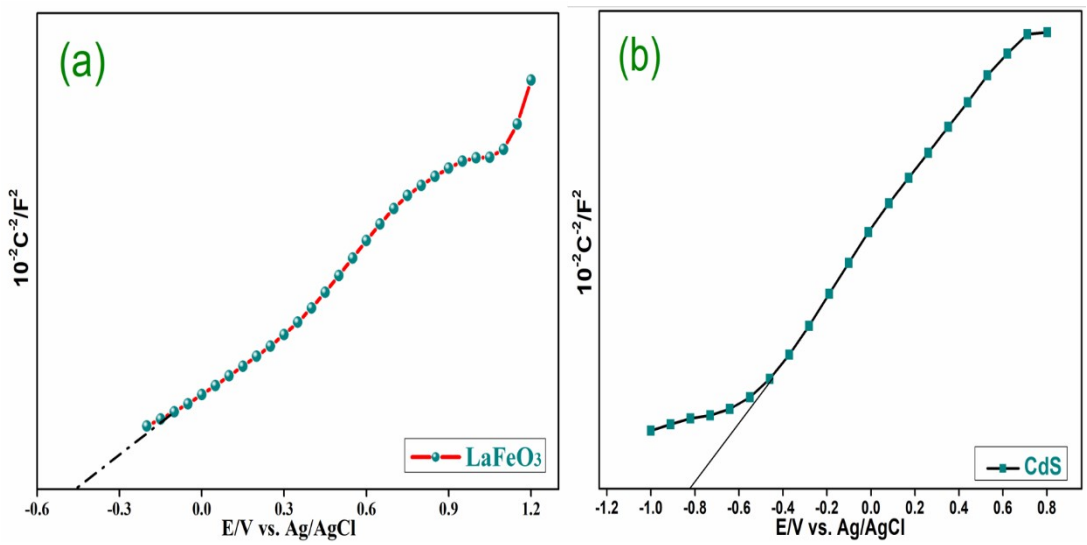

Fig S14 Mott-Schottky plot of as synthesized photocatalyst **(a)** $LaFeO_3$, **(b)** CdS.

Graphical abstract

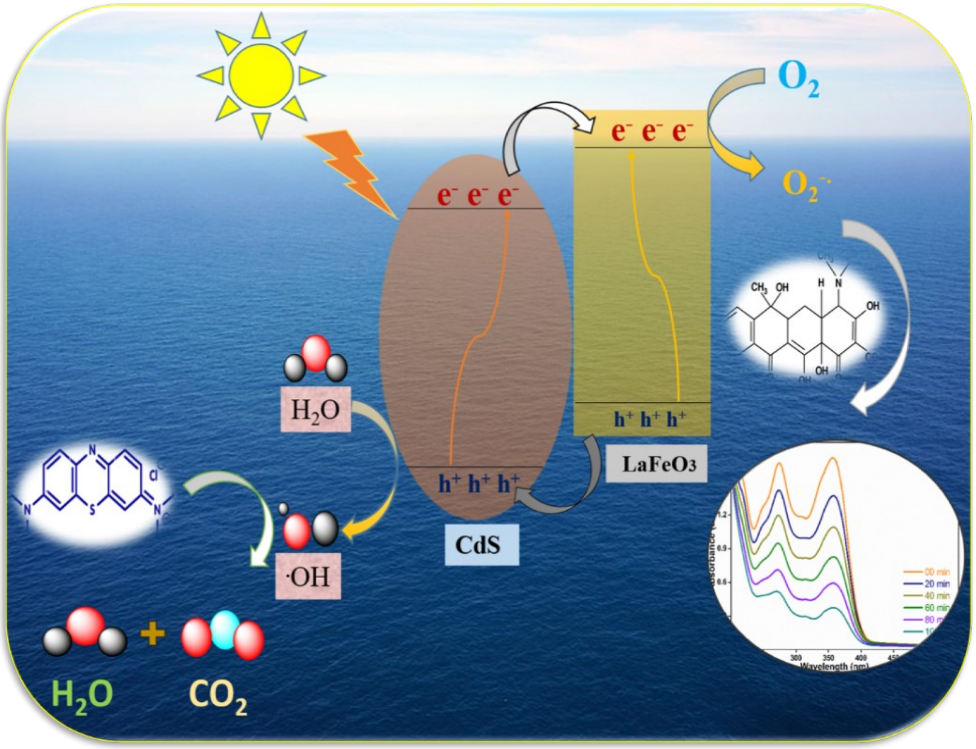

Fig S15 Abstract diagram of $LaFeO_3$/CdS heterojunction material.